system. For $D_{SL} << D_{CuKTSM2}$ the lower limit for the translational diffusion coefficient for CuKTSM2 is equal to $(60 - 95) \times 10^{-8}$ cm^2/s. Because the translational diffusion constant for 16-SASL at that temperature in DMPC is about 5×10^{-8} cm^2/s,[39] the assumption that $D_{SL} << D_{CuKTSM2}$ is appropriate.

(39) Feix, J. B.; Popp, C. A.; Venkataramu, S. D.; Beth, A. H.; Park, J. H.; Hyde, J. S. *Biochemistry* **1984**, *23*, 2293-2299.

Acknowledgment. Support of this work by NIH Grants GM35472, GM22923, and RR01008 is gratefully acknowledged. We thank Professor Shirley Schreier for showing us how to orient membranes.

EXAFS Studies on the Origin of Highly Catalytic Activity in Nickel Y Zeolite

Mitsuru Sano,* Tetsuya Maruo,† Hideo Yamatera,† Minoru Suzuki,‡ and Yasukazu Saito‡

Contribution from the Laboratory of Inorganic Chemistry, College of General Education, Nagoya University, Nagoya 464, Japan, the Department of Chemistry, Faculty of Science, Nagoya University, Nagoya 464, Japan, and the Institute of Industrial Science, University of Tokyo, Tokyo 106, Japan. *Received May 27, 1986*

Abstract: Nickel species contained in Y-type zeolite have been characterized by an EXAFS technique at each stage of catalyst preparation. When nickel ions were incorporated into the zeolite by aqueous ion exchange, a kind of "solution-like" hydrated state with Ni–O = 2.06 Å was suggested from the EXAFS analysis. After calcination, the nickel ions, surrounded by an average of 3.6 oxygen atoms with Ni–O = 2.05 Å, scattered around the exchangeable sites with unsaturated coordination. According to the EXAFS and ESCA (electron spectroscopy for chemical analysis) results, the nickel ions in this state could not be reduced completely by hydrogen. On the contrary, a different behavior of hydrogen reduction was observed after treatment of the hydrated-nickel zeolite with an aqueous sodium hydroxide solution. A new nickel hydroxide oligomer with Ni–O = 2.06 Å was formed in the supercage by this treatment. Moreover, calcination of this alkali-treated zeolite under oxygen atmosphere gave another new product containing nickel atoms with 3.5 oxygen neighbors at 2.08 Å and three second-nearest nickel neighbors at 2.99 Å. These oligomeric nickel-oxide clusters are certainly responsible for the high catalytic activity in CO oxidation. Hydrogen reduction of the small oxide clusters gave the zeolite catalyst which has an excellent activity for benzene hydrogenation. This material was confirmed to contain finely dispersed metallic nickel by the radial distribution function derived from the EXAFS spectrum.

Zeolites are crystalline aluminosilicates consisting of three-dimensional arrays of SiO_4 and AlO_4 tetrahedra. The void space enclosed within the unit is called the sodalite cage,[1] whereas a larger void space, called the supercage, is formed by linking sodalite units by hexagonal prisms. Windows 7.4 Å in diameter are formed in the supercage. This is schematically shown in Figure 1. The windows and cavities are large enough to allow small molecules to enter into the crystallite. Zeolite structures lead to many practical applications as adsorbents and catalysts. Zeolites also contain exchangeable cations, which play an important role in their catalytic activity. Zeolites containing transition metals are especially important in hydrogenation, hydrocracking, and hydroisomerization.[1] In spite of efforts to finely disperse metals in zeolites, preparation of highly active metal-containing zeolites is generally difficult.

Recently, Suzuki et al.[2] found that the catalytic activities of a nickel-exchanged Y zeolite were remarkably improved by soaking the zeolite in an aqueous NaOH solution (e.g., the activity for CO oxidation was enhanced from 4–5% conversion for the Ni Y zeolite up to more than 90% for the NaOH treated zeolite). They ascribed the enhanced activity to small nickel oxide aggregates in the zeolite, formed with the NaOH treatment. Investigation of the structural changes of the incorporated nickel and perhaps the elucidation of the mechanism of enhanced activity is undoubtedly valuable for developing methods of catalyst preparation.

EXAFS spectroscopy is used to determine the local structure around a specific atom in any phase.[3] This spectroscopic technique is well suited for tracing the structural changes during the processes of catalyst preparation. The main purpose of this work is to find out the structural change around the nickel atom induced by the treatment with a sodium hydroxide solution and to correlate the catalytic activity with the structure of active species, elucidated by use of EXAFS spectroscopy.

Experimental Section and Data Analysis

Sample Preparation. The sodium form of Linde Y-type zeolite (S-K-40) was ion exchanged with 0.1 M $Ni(NO_3)$ aqueous solution at 343 K. After filtration, the solid material was washed with distilled water to remove excess ions and then dried at 383 K (abbreviated hereafter as NiY-1). The NiY-1 sample was treated with aqueous NaOH solution of pH 10.5 for 1 h at 293 K, followed by washing and drying at 383 K in air (NiYOH-1). The amounts of nickel ions in both NiY-1 and NiYOH-1 were demonstrated by flame photometry as 8.97 and 8.55 wt %, respectively. Both samples (NiY-1 and NiYOH-1) were gradually heated up to 643 K and maintained for 3 h in the flow of 10% O_2/He (9 L/h). The products (NiY-2 and NiYOH-2) were cooled slowly down to room temperature and transferred to an EXAFS cell in the same atmosphere. Reduction in a flow of hydrogen (9 L/h) was performed at 643 K for 6 h (NiY-3 and NiYOH-3), followed by transfer in hydrogen to the EXAFS cell.

ESCA Measurement. The X-ray photoelectron spectra were recorded under 3×10^{-7} Torr (1 Torr = 133.3 Pa) or below by using a JEOL Model JESCA-3A spectrometer with aluminum $K\alpha_{1,2}$ radiation (1486.6 eV) as the X-ray excitation source. The electron binding energies were referenced to the Au $4f_{7/2}$ (83.8 eV) peak of the gold sputtered onto the sample.

* College of General Education, Nagoya University.
† Faculty of Science, Nagoya University.
‡ University of Tokyo.

(1) *Zeolite Chemistry and Catalysis*; Rabo, J. A., Ed.; American Chemical Society: Washington D.C., 1976.
(2) Suzuki, M.; Tsutsumi, K.; Takahashi, H.; Saito, Y. Internation Chemical Congress of the Pacific Basin Societies, Honolulu, 1984.
(3) Teo, B. K.; Joy, D. C. *EXAFS Spectroscopy, Techniques, and Applications*; Plenum: New York, 1981.

0002-7863/87/1509-0052$01.50/0

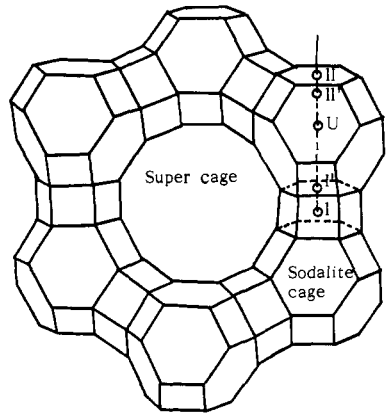

Figure 1. Cation sites and their designations in Y zeolite.

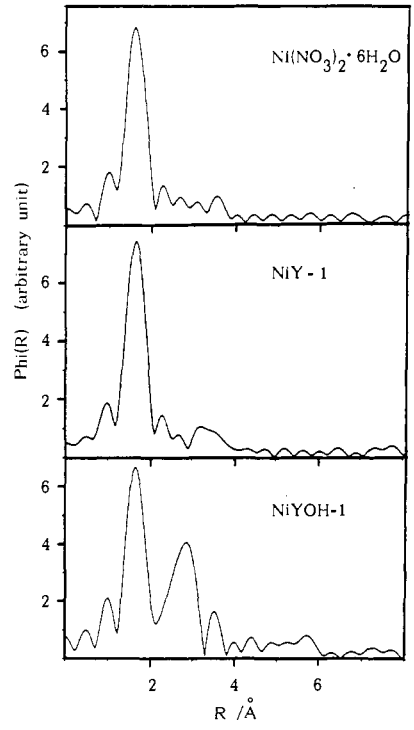

Figure 2. Fourier transforms of the EXAFS spectra of $Ni(NO_3)_2 \cdot 6H_2O$, NiY-1, and NiYOH-1.

EXAFS Measurement. The laboratory EXAFS spectrometer, basically consisting of an X-ray tube (Philips fine focus, Mo anode, 2 kW), an X-ray spectrometer with a Johann-type curved crystal (LiF 200), and an X-ray counter system, was described in detail elsewhere.[4] The X-ray source was operated at 16 kV and 7.5–12.5 mA. The average data collection time was approximately 20 h, and a signal count of over 2×10^6 was obtained in the EXAFS region. Measurements were made on each sample more than once, and no sample degradation was observed during the data acquisition time. The spectra were obtained in the range from 8060 to 8910 eV.

Data Analysis. The EXAFS spectra have been analyzed by following standard procecures.[5] The absorption background before the edge was curve-fitted by a modified Victoreen equation, $a\lambda^3 + b\lambda^4 + c$, where λ is the wavelength, and a, b, and c are variable parameters. The absorption spectrum was obtained by subtracting the calculated fitting-curve from the measured spectrum, and the resulting spectrum, $\mu(k)$ is fitted with a smoothing curve function $\mu_0(k)$ by means of a cubic spline routine. In this procedure, the absorption spectrum above the edge is divided into several regions, each of which is fitted with a third-order polynomial with a weighting scheme to account for the smaller EXAFS at higher energies. The individual polynomials are constrained to meet each other with equal slopes at the spline points and combined to form an overall curve for $\mu(k)$. Then, the EXAFS, $\chi(k)$, is obtained by $\chi(k)$

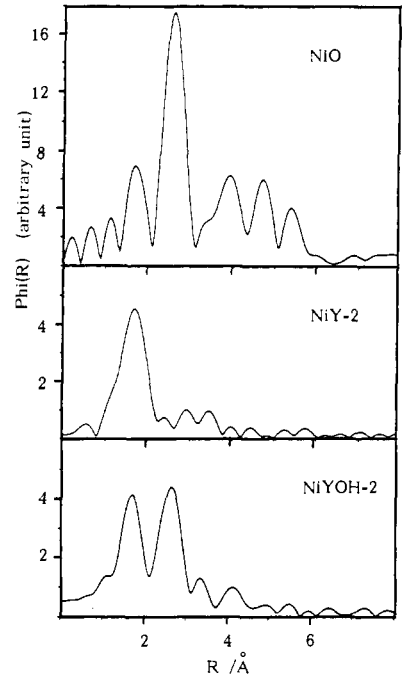

Figure 3. Fourier transforms of the EXAFS spectra of NiO, NiY-2, and NiYOH-2.

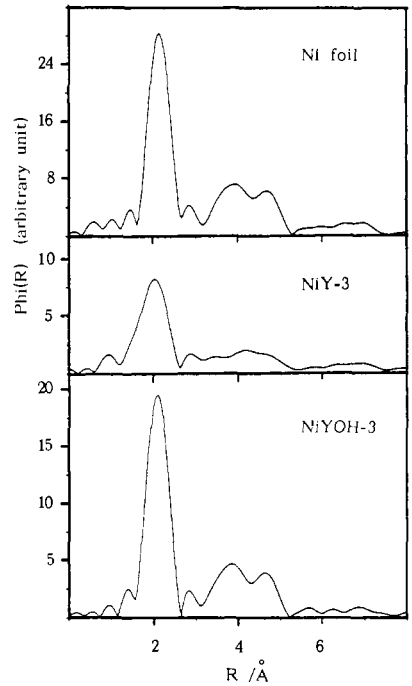

Figure 4. Fourier transforms of the EXAFS spectra of metallic Ni, NiY-3, and NiYOH-3.

$= [\mu(k) - \mu_0(k)]/\mu_0(k)$. The photoelectron wave vector is given by $k = [(E - E_0)2m/\hbar^2]^{1/2}$, where E is the photon energy and E_0 is some reference energy which does not coincide with the energy of the absorption edge.

The curve-fitting analysis was performed according to the method of Cramer et al.[6] with use of the equation

$$k^3\chi(k) = \sum c_0 N R^{-2} \exp(-c_1 k^2) k^{-c_2} \sin [a_0 + (a_1 + 2R)k + a_2 k^2]$$

where N and R represent the coordination number and the interatomic distance, respectively; c_0, c_1, and c_2 are the parameters for the amplitude functions, and a_0, a_1, and a_2 are the phase-shift parameters. We examined the spectra of the NiO and metallic Ni to determine the parameter values for Ni–O and Ni–Ni interactions.

(4) Sano, M.; Maruo, T.; Yamatera, H. *Bull. Chem. Soc. Jpn.* **1984**, *57*, 2757–2760.
(5) Cramer, S. P.; Hodgson, K. O. *Prog. Inorg. Chem.* **1979**, *25*, 1–39.
(6) Cramer, S. P.; Hodgson, K. O.; Stiefel, E. I.; Newton, N. E. *J. Am. Chem. Soc.* **1978**, *100*, 2748–2761.

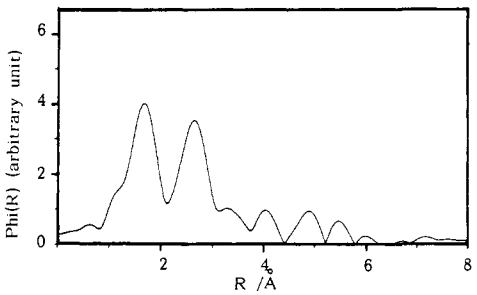

Figure 5. Fourier transform of the EXAFS spectrum of the dehydrated Ni A zeolite.

Results

Fourier transforms of the EXAFS data to real space, the $\phi(R)$ functions, at each step of the catalyst preparation are summarized in Figures 2–4 together with those of reference compounds. These correspond to a kind of radial distribution function around the nickel atom including correction of the phase-shift. (The atoms flatly scattered in distance from the nickel atom, due to disorders or vibrations, are depreciated or even ignored in these "radial distribution functions".) Figure 2 shows results on the Ni Y zeolites (NiY-1 and NiYOH-1) and solid $Ni(NO_3)_2 \cdot 6H_2O$. The Fourier transform of the EXAFS of NiY-1 exhibits a single peak at about 1.7 Å (the value before the phase-shift correction) and is similar to that of $Ni(NO_3)_2 \cdot 6H_2O$ containing $[Ni(H_2O)_6]^{2+}$. On the other hand, the NaOH-treated NiYOH-1 gave two peaks at about 1.7 and 2.8 Å. The former peak is probably the same in origin as that of NiY-1. The dehydrated NiY-2 and NiYOH-2 were compared with NiO in Figure 3. Fourier transformation of the NiO EXAFS gave four peaks at 1.7, 2.6, 3.8, and 4.7 Å, corresponding to the Ni–O, Ni–Ni, Ni–O and/or Ni–Ni, and Ni–Ni distances, respectively. As for both NiY-2 and NiYOH-2, a peak was found at the same position as the first peak of NiO, but with a lower intensity. Furthermore, NiYOH-2 gave another peak at 2.6 Å nearly identical with the Ni–Ni distance in NiO. Figure 4 shows the results on the reduced NiY-3 and NiYOH-3 together with the spectrum of a thin Ni foil. Though the intensity of the main peak for NiYOH-3 was lower than that for the metal, the position of the peak coincided well with that of Ni foil. However, it is to be noted that the radial distribution for NiY-3 is different from those for Ni foil and NiYOH-3.

Discussion

The structure of transition metals incorporated in A zeolite has been studied by EXAFS[7,8] and X-ray diffraction.[9] The Fourier transform of the EXAFS for cobalt and manganese A zeolite was determined precisely by Morrison et al.[7,8] In order to examine the reliability of our EXAFS results, the Fourier transform, $\phi(R)$, for NiNaA dehydrated in vacuum was obtained (Figure 5). The main peak was found at about 1.7 Å and another peak with a slightly lower intensity at 2.7 Å (before phase-shift correction). These results are consistent with the previous paper.[8] (The intensity of the second peak is greater in our result than in those of Morrison et al.) The coordination number, N, and the atomic distance, R, were determined from our EXAFS result, where the first peak was back-Fourier transformed by use of a proper window and the resulting curve was subjected to the curve-fitting analysis.[6] The results of $N = 3.1$ and $R_{Ni-O} = 2.04$ A are consistent with the conclusion of trigonal coordination from the EXAFS analysis[7,8] of Morrison et al. as well as from the X-ray crystal structure analysis.[9] According to the X-ray diffraction of cobalt A zeolite,[9] the cobalt cations are located along the (111) axis passing through the center of the hexagonal rings, displaced 0.34 Å out of the plane of the three nearest oxygen atoms. The second EXAFS peak at 2.7 Å (before phase-shift correction) is attributable to the silicon, aluminum, and remaining oxygen atoms in the hexagonal ring. These results demonstrate that the backscattering from the zeolite framework is observable in the EXAFS spectrum for the metal ion fixed at the site.

Hydrated Nickel Y Zeolite. The only peak found in the $\phi(R)$ curve of hydrated NiY-1 is attributed to coordinated oxygen atoms, because the same peak is observed for solid $Ni(NO_3)_2 \cdot 6H_2O$. The coordination number of 5.9 and the Ni–O distance of 2.06 Å, determined from the curve-fitting analysis, are very close to the corresponding values[10] in $[Ni(H_2O)_6]^{2+}$. Since no second peak was found, nickel contained in Y zeolite will certainly exist as the hydrated Ni^{2+} ion coordinated with six oxygen atoms, similar to the "solution-like" Co^{2+} ion of $Co_{18.2}Na_{20.7}Y \cdot xH_2O$ as reported by Morrison et al.[8] A large void space such as the supercage will be required for these "solution-like" bulky hydrated Ni^{2+} ions (Figure 1).

The Fourier transform of the NiYOH-1 EXAFS spectrum gave two peaks at 1.7 and 2.8 Å (before phase-shift correction). The first peak is ascribed to six oxygen atoms surrounding the nickel ions, since it appears at the same position ($R_{Ni-O} = 2.06$ Å) as that of NiY-1 and of the reference $Ni(NO_3)_2 \cdot 6H_2O$ with an intensity corresponding to $N = 5.4$. The second peak observable for NiYOH-1 corresponds to either Ni–Ni or Ni–zeolite framework (including Ni–Al, Ni–Si, and Ni–O). If the second peak appeared by the interaction of nickel with the Y-zeolite framework, the nickel ion would be located at the S_I site with nearly perfect octahedral coordination surrounded by the six framework oxygen atoms and by Al and Si atoms as the second nearest neighbors. However, the reported Ni–O distances for the nickel atoms at the S_I site of nickel faujasite[11] are 2.29 Å, distinctly different from the observed Ni–O distance of 2.06 Å. Since nickel hydroxide in an aqueous alkaline solution is easy to polymerize by forming Ni–OH–Ni linkages, the second peak is more likely assigned to the Ni–Ni interaction. During the NaOH treatment of the nickel Y zeolite, the nickel ions would coagulate to form a small nickel hydroxide oligomer in the large space of the supercage. Thus the second peak at 2.8 Å (before phase-shift correction) is attributed to Ni–Ni interaction in the nickel hydroxide oligomer.

Dehydrated Nickel Y Zeolite. The calcined nickel Y zeolite, NiY-2, gave only one peak assigned to Ni–O ($R_{Ni-O} = 2.05$ Å and $N = 3.6$). Dehydration causes little change in the position of the peak but a dramatic decrease in its intensity; the latter suggests a decrease in the number of coordinated oxygen atoms. This EXAFS result might be inconsistent with the result of a single-crystal X-ray diffraction analysis[11] of the dehydrated nickel faujasite, since most of the nickel ions are preferentially situated according to the X-ray results at the center of hexagonal prism (S_I site) with octahedral coordination at $R_{Ni-O} = 2.289$ Å, while the remaining nickel ions are situated at the S_I', S_{II}, and S_{II}' sites with trigonal or tetrahedral coordination. However, it is conceivable that the nickel ions at the S_I site are statically or dynamically displaced and the X-ray diffraction analysis has given the space- or time-averaged position of the nickel ions, whereas our EXAFS results are concerned with the individual and instantaneous local structure around each nickel ion. Thus the shorter distance of $R_{Ni-O} = 2.05$ Å and the lower coordination number of $N = 3.6$ from EXAFS are compatible with the larger values of 2.289 Å and 6 from X-ray diffraction,[11] respectively. Since the second-neighbor shells of framework oxygen, aluminum, and silicon atoms are presently observed in dehydrated NiA as in CoA,[8] the absence of any second peak of significance in the spectrum of dehydrated NiY-2 zeolite may suggest that the second-nearest neighbors are scattered in distance from the nickel ion. This situation is different from that observed in dehydrated

(7) Morrison, T. I.; Reis, A. H., Jr.; Gebert, E.; Iton, L. E.; Stucky, G. D.; Suib, S. L. *J. Chem. Phys.* **1980**, *72*, 6276–6282. Morrison, T. I.; Iton, L. E., Shenoy, K.; Stuckey, G. D.; Suib, S. L.; Reis, A. H., Jr. *J. Chem. Phys.* **1980**, *73*, 4705–4706.

(8) Morrison, T. I.; Iton, L. E.; Shenoy, G. K.; Stucky, G. D.; Suib, S. L. *J. Chem. Phys.* **1981**, *75*, 4086–4089.

(9) Yanagida, R. Y.; Vance, T. B., Jr.; Seff, K. *Inorg. Chem.* **1974**, *13*, 723–727. Riley, P. E.; Seff, K. *Inorg. Chem.* **1974**, *13*, 1355–1360.

(10) Ohtaki, H.; Yamagauchi, T.; Maeda, M. *Bull. Chem. Soc. Jpn.* **1976**, *49*, 701–706.

(11) Olson, D. H. *J. Phys. Chem.* **1968**, *72*, 4366–4373.

(12) Gallezot, P.; Imelik, B. *J. Phys. Chem.* **1973**, *77*, 652–656.

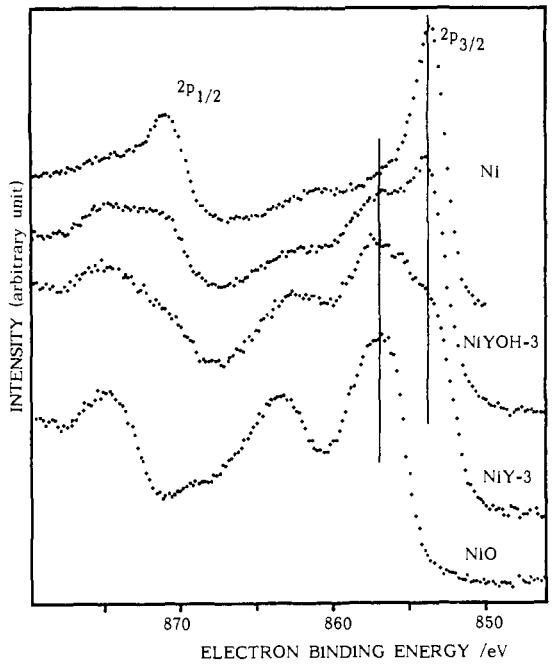

Figure 6. ESCA spectra of metallic Ni, NiYOH-3, NiY-3, and NiO.

NiA. The experimental evidence shows that nickel ions in NiY-2 exist separately with unsaturated oxygen coordination, although their exact location cannot be determined.

On dehydration of NiYOH-1 (to form NiYOH-2), the first peak remained unchanged in position, but the second peak shifted from 2.8 to 2.6 Å (before phase-shift correction). Since nickel ions are easily polymerized in aqueous alkaline solution with Ni–OH–Ni linkages, the air calcination leads to the formation of nickel oxide. The EXAFS parameters are fitted to the structure of NiO crystallite determined by X-ray diffraction: the first- and second-neighbor shell distances, R_{Ni-O} = 2.084 Å and R_{Ni-Ni} = 2.947 Å, and the coordination numbers, N_{Ni-O} = 6 and N_{Ni-Ni} = 12, respectively. With NiO adopted as the reference, the EXAFS spectrum of NiYOH-2 was analyzed to have the neighbor-shell distance and the coordination number of R_{Ni-O} = 2.08 Å and N_{Ni-O} = 3.5 for the first peak and R_{Ni-Ni} = 2.99 Å and N_{Ni-Ni} = 3.4 for the second, respectively. These EXAFS results show that the nickel oxide species existing in NiYOH-2 is obviously different from NiO crystallite in the numbers of the first and second neighbors of each nickel atom. The third- and fourth-neighbor shells, observed in NiO crystallite, were not observed with significance in NiYOH-2. These findings suggest that noncrystalline and small nickel oxide aggregates are formed in NiYOH-2. In a previous study,[2] no peaks corresponding to NiO crystalline were found in the X-ray diffraction spectrum of a sample from the same treatment of NiYOH-1 as that for the present study, and no NiO particles were observed by high-resolution electron microscopy. The present EXAFS results together with the previous ones suggest that the oligomeric NiO aggregates, which are so small as to escape X-ray diffraction and electron microscopic detection and are not easily obtainable in aqueous nickel salt solution, were formed inside the zeolite cavity by such a simple procedure as the NaOH treatment of nickel-containing zeolite. Oligomeric clusters of nickel oxide, highly dispersed in the zeolite, would account for the excellent and unique catalytic activity of NiYOH-2 for CO oxidation in contrast to the isolated nickel ions in NiY-2, which showed only a low activity.[2] It is quite conceivable that the oligomeric cluster is located inside the supercage, since it is larger than 7 Å in diameter and can contain more than four nickel atoms.

Reduced Nickel Y Zeolite. The EXAFS result (R_{Ni-Ni} = 2.51 Å, N = 8.0) of NiYOH-3 is very similar to that of Ni foil, since the Ni–Ni distance is the same as that of nickel metal. The rather small coordination number of 8.0 indicates, however, that fine nickel metal particles are formed from the oligomeric nickel oxide located inside the supercage.

The Fourier transform of the NiY-3 EXAFS spectrum shows the nickel metal peaks to be lower than those for metal foil and for NiYOH-3. A shoulder observed at 1.7 Å (before phase-shift correction) would probably be due to Ni–O interactions. These features of the Fourier transform show that the nickel ions are not completely reduced in NiY-3 and a considerable amount of isolated nickel ions are still left combined with the zeolite-framework oxygen atoms.

In order to support the present interpretation, ESCA measurements were carried out for NiY-3, NiYOH-3, NiO, and Ni metal (Figure 6). In the Ni $2p_{3/2}$ binding-region, the major peak of NiO was observed at 856.0 eV, accompanied by the shake-up satellite at 863.2 eV; the reference is the metal $2p_{3/2}$ peak at 853.6 eV. The intense peak of NiYOH-3 at 854.2 eV is assigned to nickel metal, and accompanying weak peaks at higher energies are attributed to nickel oxide. Thus the reduced, alklai-treated nickel Y zeolite was found to contain metallic nickel together with a small amount of NiO based on both ESCA and EXAFS data. In the ESCA spectrum of NiY-3, on the other hand, the intensity of the metal peak (853.6 eV) is low and the major signal appears at the oxide region (856.0 eV). This shows that nickel ions were only partly reduced in NiY-3 under the present experimental conditions in agreement with the EXAFS observation.

As reported previously,[2] the catalytic activity of NiY zeolite for benzene hydrogenation was tremendously enhanced by the NaOH treatment from 4–5% conversion up to more than 90%. Since the difference between NiY-3 and NiYOH-3 in the extent of nickel ion reduction is evident from EXAFS, the activity enhancement is well interpreted in terms of the formation of finely dispersed metallic nickel.

Conclusion

Useful information was obtained from the EXAFS study about the structural changes occurring in NaOH treatment, calcination, and reduction of nickel ions incorporated in Y zeolite. The nickel ions contained in the hydrated Y zeolite have the $[Ni(H_2O)_6]^{2+}$ structure, or a "solution-like" structure, located in the supercage. By calcining the hydrated zeolite, a part of the isolated nickel ions would migrate into the hexagonal prism, since the nickel ions in hexagonal prisms are hardly reduced by the conventional heating procedure in hydrogen atmosphere.[13] The hydrolysis of the "solution-like" nickel ions and the formation of oligomeric hydroxide with Ni–OH–Ni linkages are attained by the NaOH treatment. The oligomeric nickel hydroxide, located in the supercage due to its large size, is changed by calcination into unique oligomeric nickel oxide in the supercage. This unique and small oligomeric nickel oxide can be converted into fine nickel metal particles by hydrogen reduction. The excellent catalytic activities for CO oxidation and benzene hydrogenation obtained by the NaOH treatment of nickel Y zeolite were ascribed to the structural change in the incorporated nickel. Application of similar techniques to other transition metal species is expected to be useful in catalyst preparation.

Acknowledgment. One of the authors (M.S.) thanks the Ishida Fundation for financial support. He also acknowledges a Grant-in-Aid (No. 59740295) for Scientific Research from the Ministry of Education, Science and Culture.

(13) Suzuki, M.; Tsutsumi, K.; Takahashi, H. *Zeolites* **1982**, *2*, 51–58.